List of Tables

List of Figures

Supplementary analysis for Section 3.2 is provided as follows:

- Since our meteorological adjustments are made by colocating ozone and dewpoint observations (when selecting subsamples, meteorological variables used in different sampling schemes are coupled with ozone data. I.e., not only ozone but also dewpoint is varying in the sampling analysis), we conduct a further sensitivity test by fitting the same ozone data, but using different sources of dewpoint measurements, including: (1) coupled daily data, (2) monthly averages of all daily nighttime data, and (3) monthly averages of all 24-h hourly data. We randomly selected 4 days-per-month to carry out this test by 1000 iterations. The result shows much lower residual RMSD and MAD are obtained from the coupled data, followed by monthly nighttime averages, and 24-h averages have the greatest errors (see Figure S7, note that ENSO index is only available at monthly scale and thus has no effect on this test). Therefore, it makes a strong evidence that a better correlation and predictive performance can be achieved by colocating ozone and meteorological variables at a finer scale.

- In Figure 2 we demonstrate that the sampling bias from weekly samples has a smaller impact on temperature trends at MLO. We show the extended result by different time periods and by each day of the week in Figure S8 (trends for meteorological variables are based on basic model (M1)). As expected, although some variability is shown in trends from weekly subsamples, the result is more consistent between different days of the week.

- Although our focus is the effect of sampling bias on ozone trends, it is also desirable to carry out the similar attribution analysis to the pure sampling deviations (defined as the differences between ozone daily value and its monthly mean). By removing the ozone variability and accounting for meteorology, we aim to identify any remaining patterns (see Table S2 for the regression output). The result shows that some seasonal differences are present and a higher sampling variability is more likely to occur from July to November. As expected, neither a clear difference between days of the week nor a trend was found in the sampling deviations. Overall, a moderate low R^2 of 0.39 was found, indicating that a large portion of the sampling deviations might merely be random noise.

Supplementary analysis for Section 3.4 is provided as follows:

- To better understand the diverse result between monthly mean bias decreases and trend bias increases in Strategy C, Figure S11 demonstrates one of the most extreme cases in MAM: We first show the contrast of time series between full sampling and Friday sampling, and then show another scenario that a time series is produced from a mixture from full sampling for MAM and Friday sampling for other months. Under this particular circumstance, we show that the trends are consistent between full and once-per-week sampling, but the trend bias turns out to be inflated if we deliberately increase samples in MAM. On the other hand, even though sampling enhancement in MAM tends to cause a low bias in the overall trends (Figure 7), we show that a very high bias could also occur by simply selecting a different day of the week sampling (Figure S12). Therefore, the direction of trend bias is not necessarily connected to the seasonal variability.

Table S-1: A list of the months that have not met the 50% data coverage criterion (MLO ozone record).

Year	Month	# daily values
1984	Apr	0
1987	Apr	0
1987	May	0
1987	Jun	0
1987	Jul	8
2000	Sep	0
2002	May	14
2003	Aug	14
2004	Dec	10
2005	Jan	0
2005	Feb	0
2005	Mar	8

Table S-2: Numerical output from the multiple regression fit to the sampling deviations (differences between daily ozone value and its monthly mean), where each month and day of the week are treated as discrete factors (e.g., to investigate which months are more likely to have a stronger sampling variability).

	Estimate	Std. Error	SNR	P-value
Intercept [ppbv]	-1.99	1.13	-1.76	0.08
trend [ppbv/dec.]	<0.01	0.09	0.04	0.97
dewpoint [°C]	-0.53	0.03	-18.65	<0.01
relative humidity [%]	-0.09	0.01	-8.42	<0.01
temperature [°C]	-0.89	0.05	-17.62	<0.01
wind direction [degree]	-0.01	<0.01	-3.03	<0.01
wind speed [m/s]	-0.04	0.03	-1.37	0.17
factor(Feb) [ppbv]	-0.04	0.41	-0.10	0.92
factor(Mar) [ppbv]	1.22	0.40	3.05	<0.01
factor(Apr) [ppbv]	0.21	0.40	0.52	0.60
factor(May) [ppbv]	2.07	0.41	5.06	<0.01
factor(Jun) [ppbv]	2.70	0.42	6.36	<0.01
factor(Jul) [ppbv]	4.81	0.42	11.34	<0.01
factor(Aug) [ppbv]	5.90	0.44	13.55	<0.01
factor(Sep) [ppbv]	5.15	0.43	11.91	<0.01
factor(Oct) [ppbv]	4.33	0.41	10.50	<0.01
factor(Nov) [ppbv]	3.83	0.41	9.43	<0.01
factor(Dec) [ppbv]	1.32	0.40	3.29	<0.01
factor(Mon) [ppbv]	-0.11	0.30	-0.35	0.73
factor(Tue) [ppbv]	-0.49	0.30	-1.61	0.11
factor(Wed) [ppbv]	-0.34	0.30	-1.12	0.26
factor(Thu) [ppbv]	-0.10	0.30	-0.34	0.73
factor(Fri) [ppbv]	-0.33	0.30	-1.10	0.27
factor(Sat) [ppbv]	-0.10	0.30	-0.33	0.74

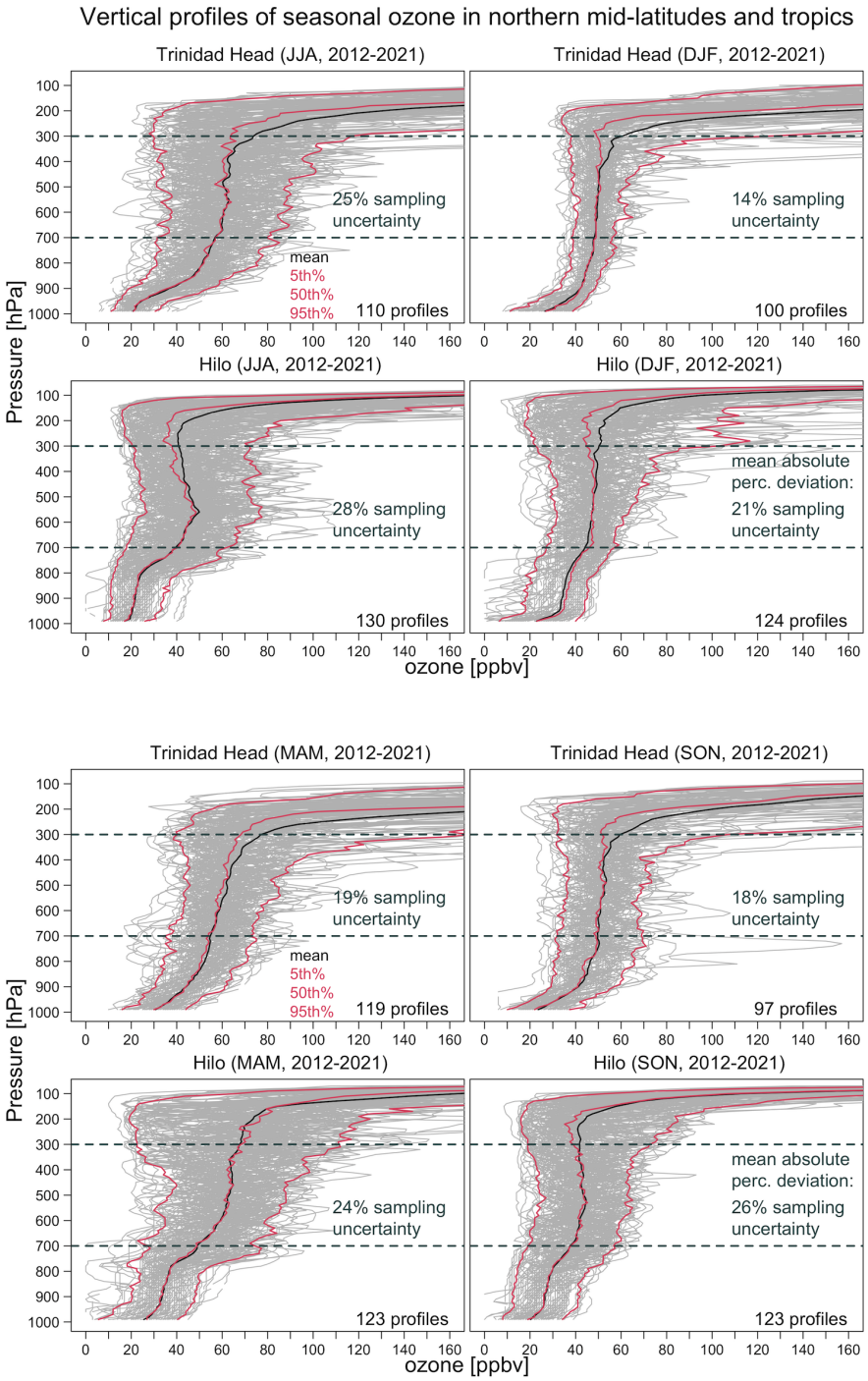

Figure S-1: Vertical profiles of seasonal ozone in the northern mid-latitudes (Trinidad Head, California) and the tropics (Hilo, Hawaii) over 2012-2021: gray lines represent individual sondes, black lines represent the mean, and red lines represent the 5th, 50th and 95th percentiles. Sampling uncertainties are evaluated by mean absolute percentage deviation at 10 hPa resolution layers within 700-300 hPa.

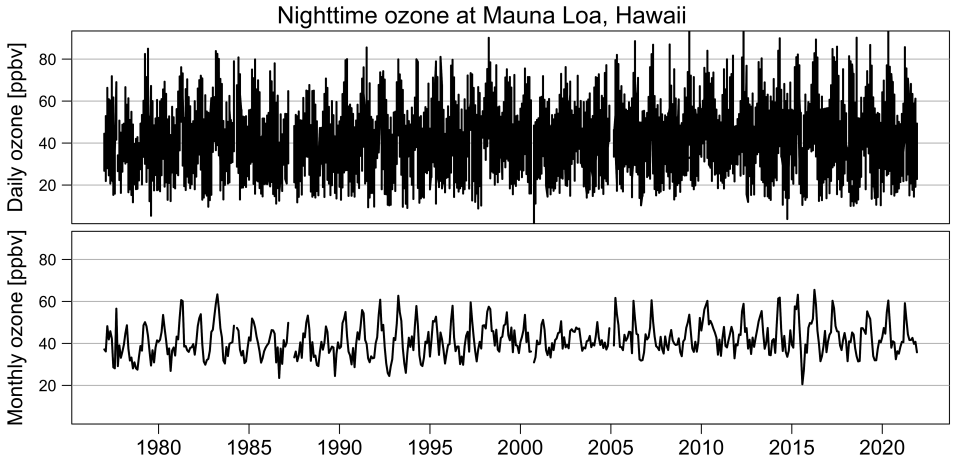

Figure S-2: Daily and monthly nighttime ozone mean time series at Mauna Loa, Hawaii.

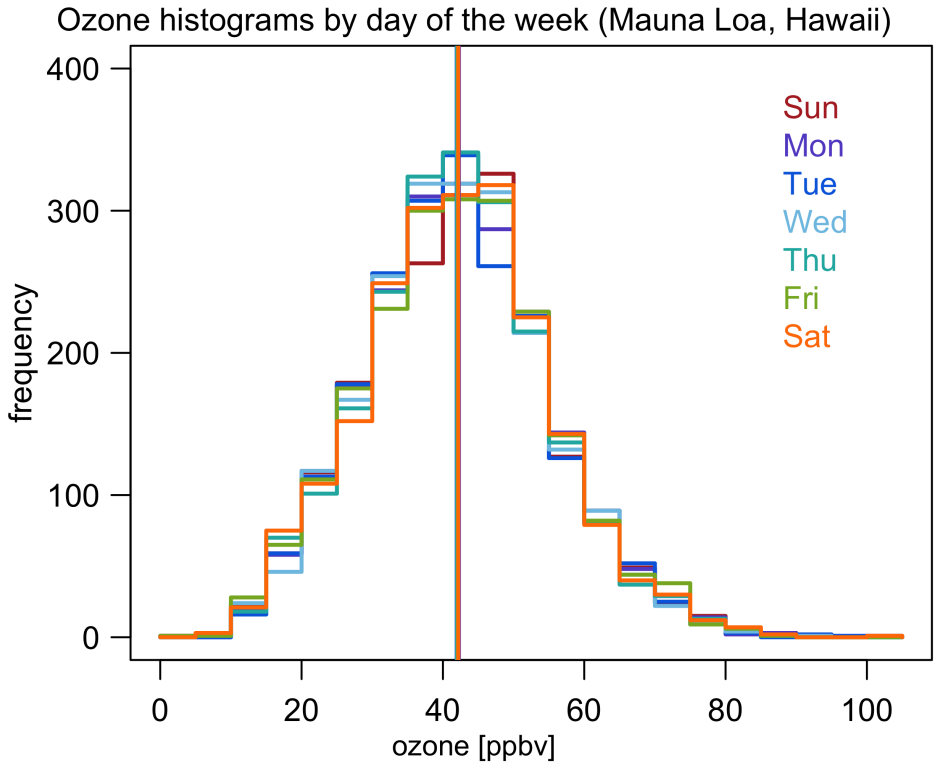

Figure S-3: Daily nighttime ozone histograms by each day of the week at Mauna Loa, Hawaii. No distinguishable difference can be observed in the average of each histogram (as indicated by the vertical line).

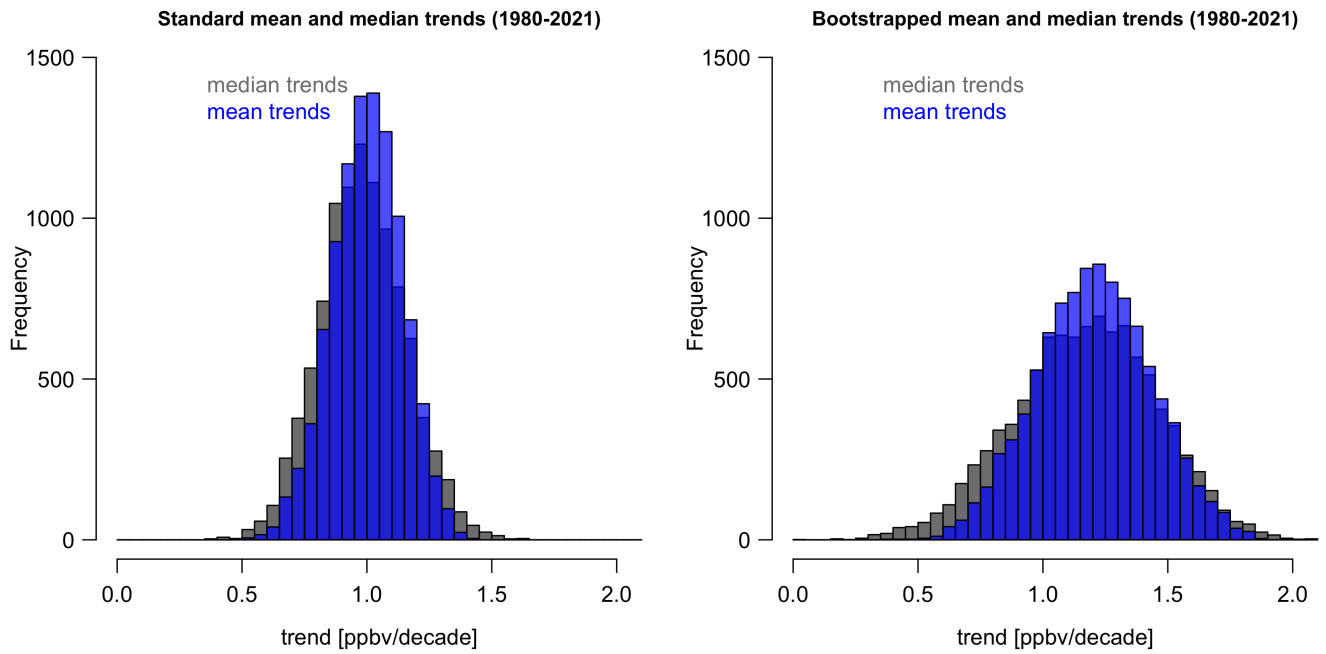

Figure S-4: Resampling distributions of the median/mean trends based on standard LAD/OLS fits (left) and moving block bootstrap (right). A total of 10,000 iterations is made and for each iteration, 4 samples per month are randomly selected and then the median/mean trends are fitted to the same subsamples. The result shows that the mean-based regression tends to have a narrower uncertainty than the median-based regression, and moving block bootstrap (accounted for autocorrelation) tends to have a greater uncertainty than the standard regression fits. Trends and associated uncertainty estimates are meteorologically adjusted (MLO nighttime ozone, 1980-2021).

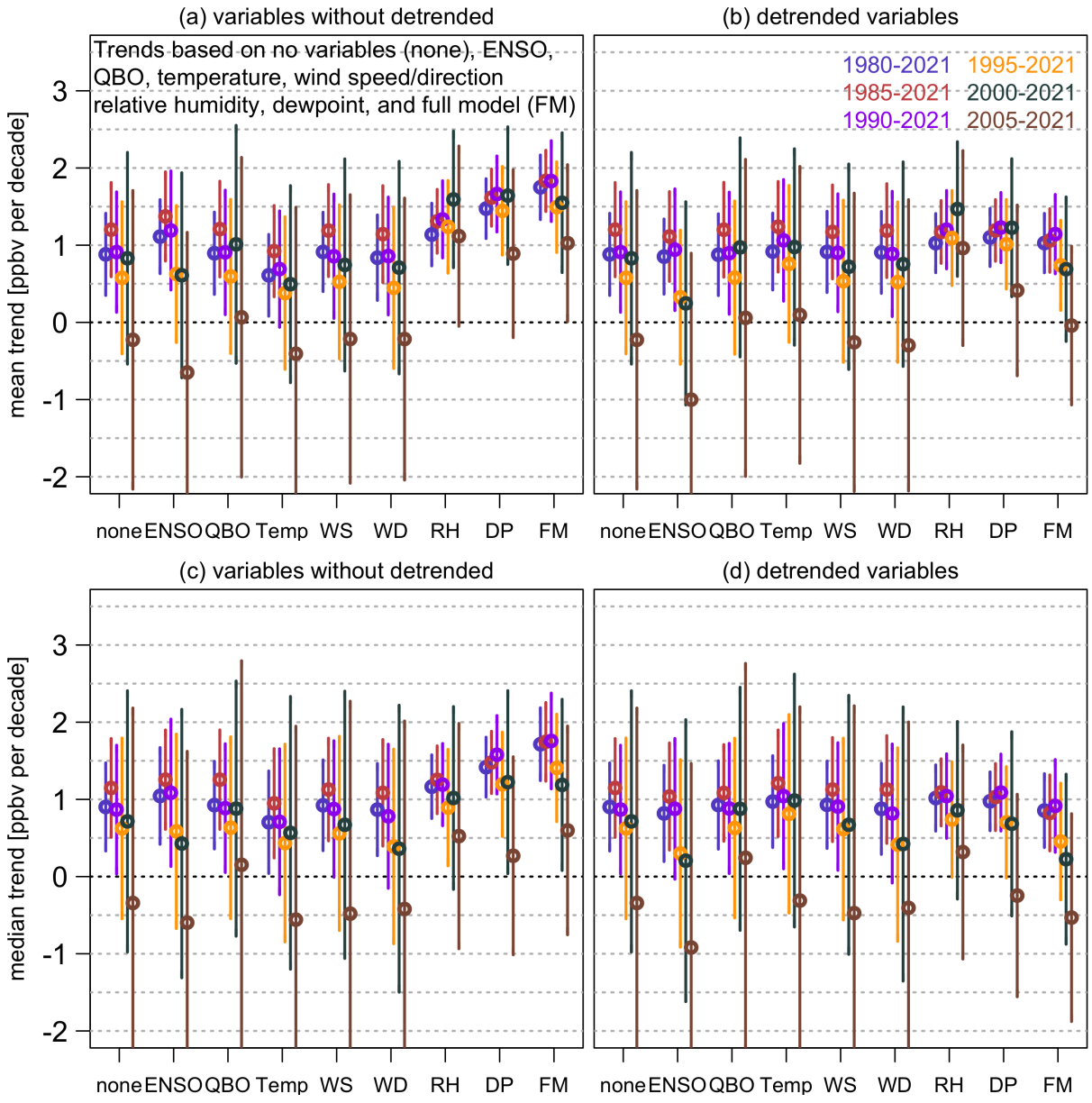

Figure S-5: Comparison of the impact of climate indices and meteorological variables on MLO ozone trend estimates and 2-sigma intervals: Ozone trends are based on the mean (a & b) and median (c & d) estimators, and derived from variables without detrended (a & c) and detrended variables (b & d), respectively. In each panel the results are based on the basic model (left), each individual variable (middle), and full model (right), as well as different time periods. Variables include El Niño-Southern Oscillation (ENSO), quasi biennial oscillation (QBO), temperature, wind speed (WS), wind direction (WD), relative humidity (RS), and dewpoint (DP). Note that the peak correlation between ENSO and ozone is found where the ENSO index shifts forward by 5 months, so here a lagged ENSO correlation is considered, albeit no noticeable impact on trends is found when using the peak or zero-lag ENSO correlation (not shown).

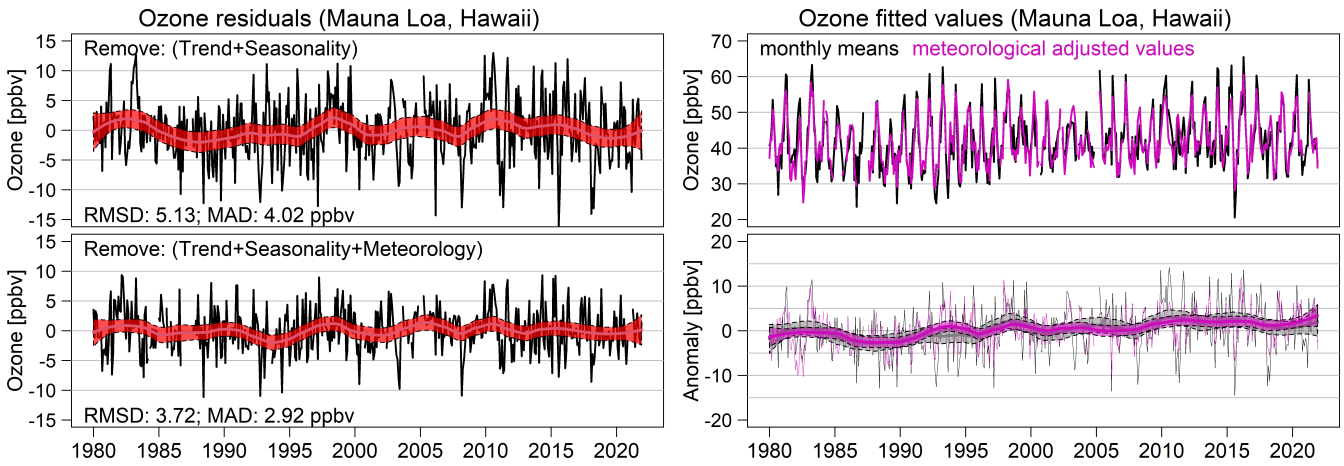

Figure S-6: Residuals from least squares regression models without and with meteorological adjustments (left), and meteorological adjusted ozone values and anomalies (right). Shaded curves indicate the Lowess smoother [$\pm$ 2-σ].

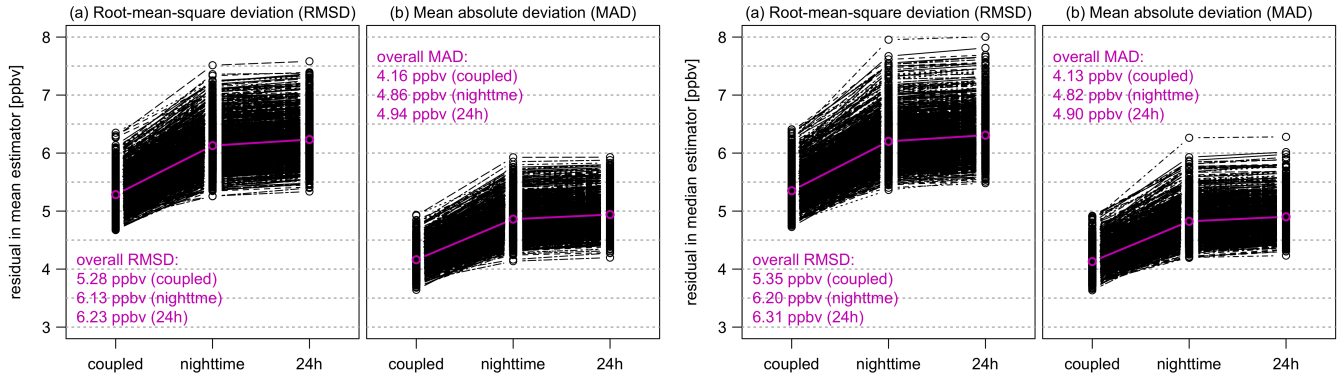

Figure S-7: RMSD and MAD from different sources of meteorological observations, based on the mean (left) and median (right) estimators: Trend models are fitted through meteorological variables selected from colocated sampling dates (coupled), from all nighttime averages (nighttime), and from all hourly averages (24h), respectively. Each black line represents an outcome from resampled data, and the purple line represents the average over 1000 iterations. The result shows a better predictive performance can be achieved by colocating dependent and independent variables at a finer scale.

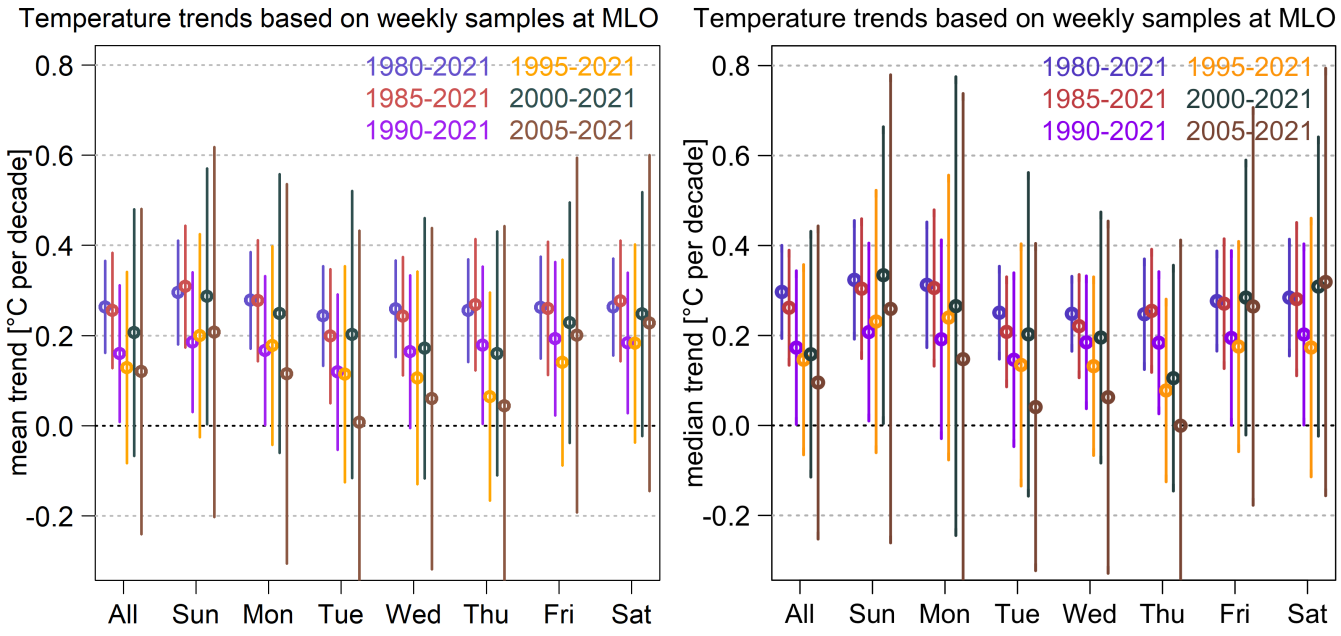

Figure S-8: MLO nighttime temperature trends based on the mean (left) and median (right) estimators.

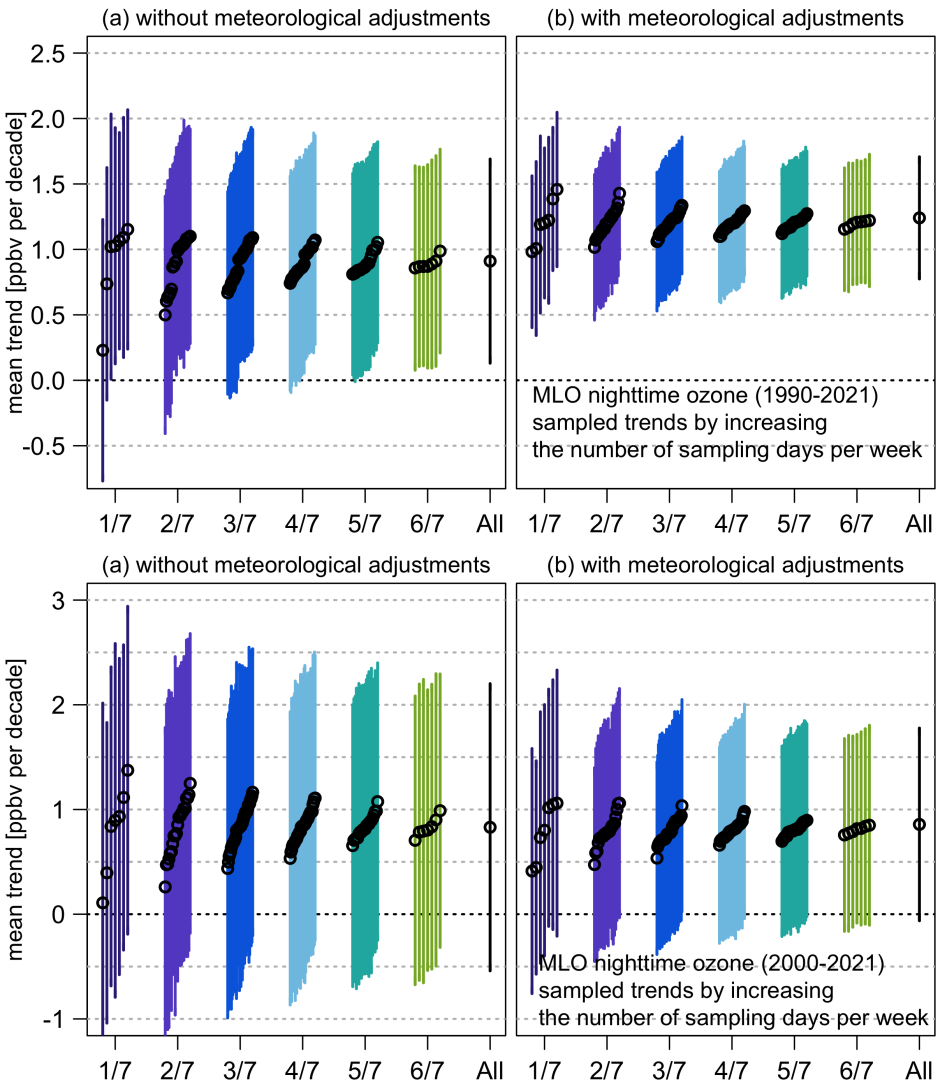

Figure S-9: Impact of increasing weekly sampling frequency on trends over 1990-2021 (upper panel) and 2000-2021 (lower panel): The possible combinations are different for each sampling scheme (i.e., a total of 7 sets for 1 day/week and 6 days/week, 21 sets for 2 days/week and 5 days/week, and 35 sets for 3 days/week and 4 days/week). For each scheme, results are sorted from the lowest to the highest sampled trend values (MLO nighttime ozone).

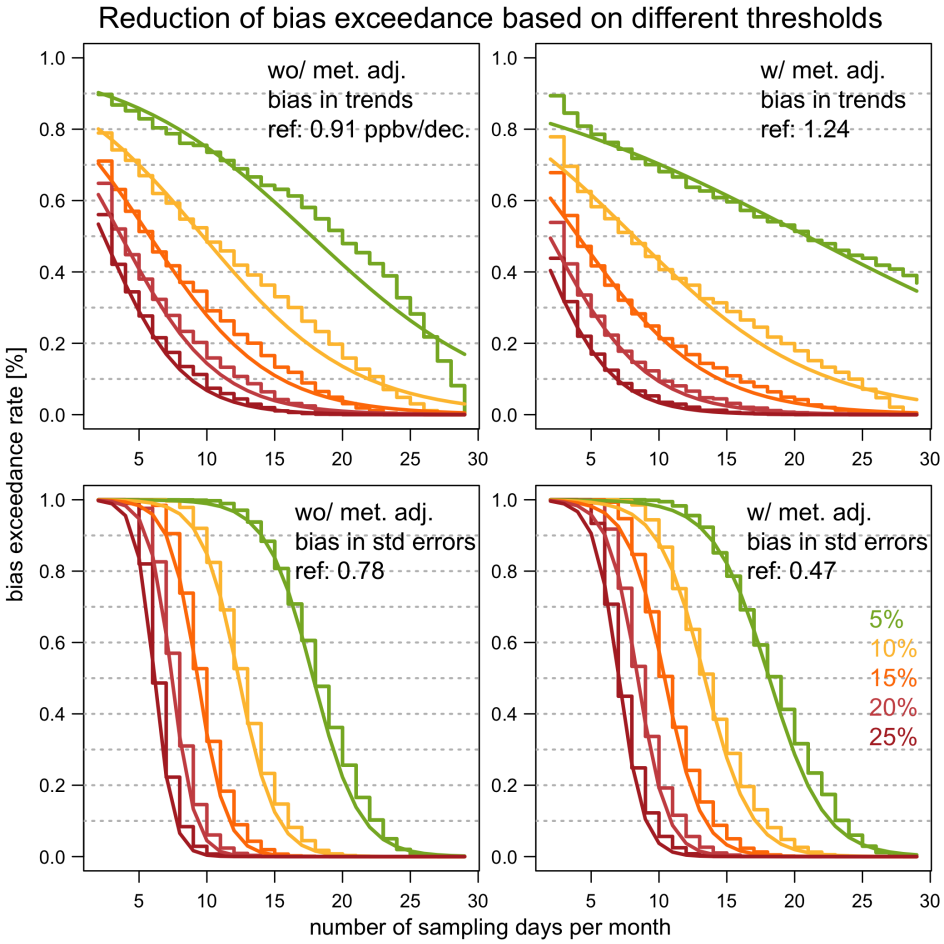

Figure S-10: Same as Figure 6, but based on without (left) and with (right) meteorological adjustments. The bias exceedance rates in each panel are estimated based on different reference numbers. For example, the green curve in the upper left panel is determined by how often do $|s_{k,x} - 0.91|/0.91$ exceeds 0.05 in 10,000 resampling (where $s_{k,x}$ is the bootstrapped trend value, $k = 1, ..., 10000$ iterations and $x = 2, ..., 29$ days/month). This result demonstrates that since there is an uncertainty in the colocated meteorological variables, the marginal decrement for the 5% bias exceedance rate is less efficient when the sampling frequency increases (but the other metrics are not affected).

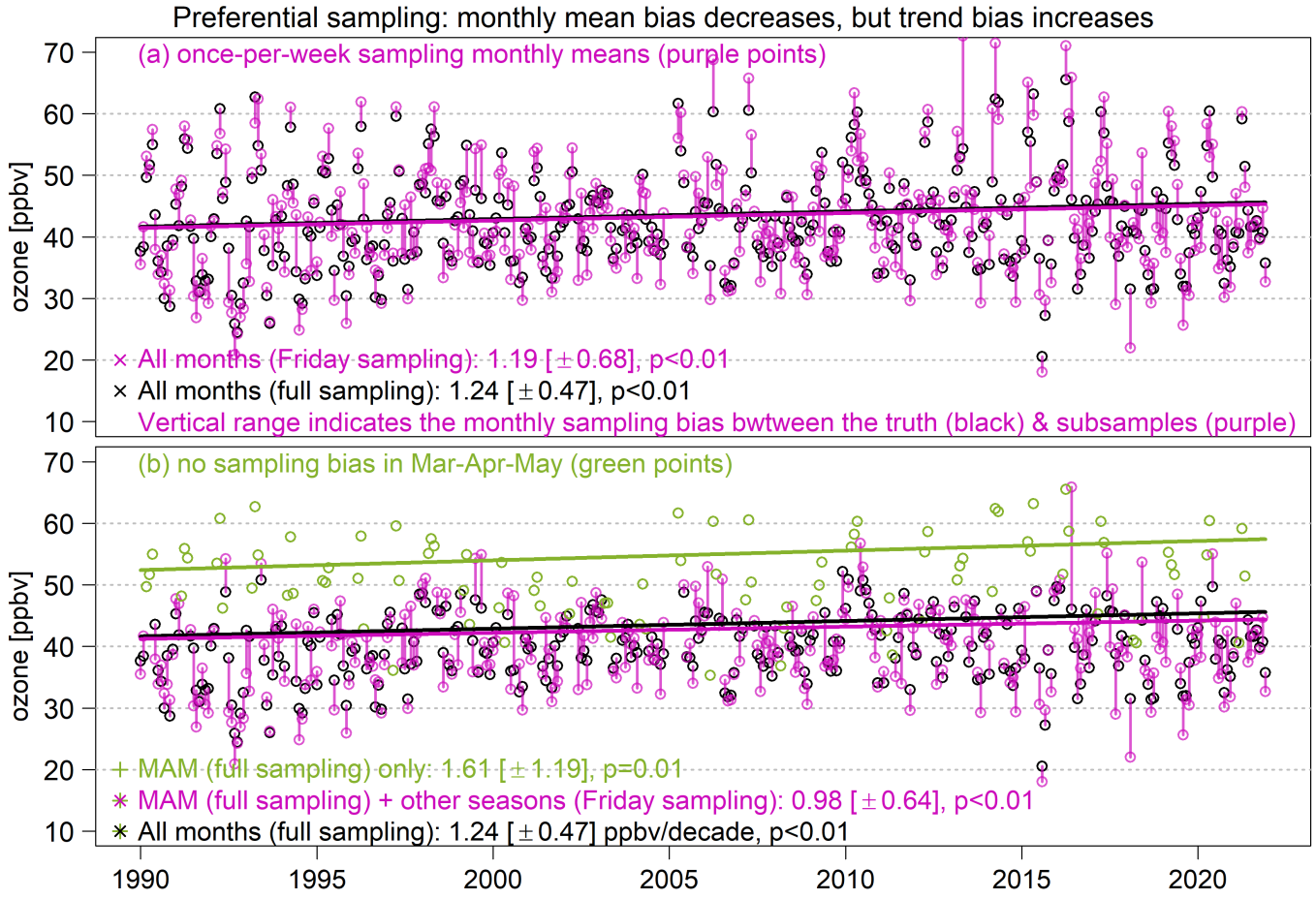

Figure S-11: Demonstration of preferential sampling for ozone time series: The upper panel shows the magnitude of monthly sampling bias between full sampling (black) and once-per-week sampling on Friday (purple). The lower panel is based on the same scheme, but under the assumption of no sampling bias in monthly means over Mar-Apr-May (green). Trends and associated uncertainty estimates are meteorologically adjusted. This example indicates that if we deliberately enhance sampling during certain months, imbalanced sampling can result in a stronger bias in the overall trend.

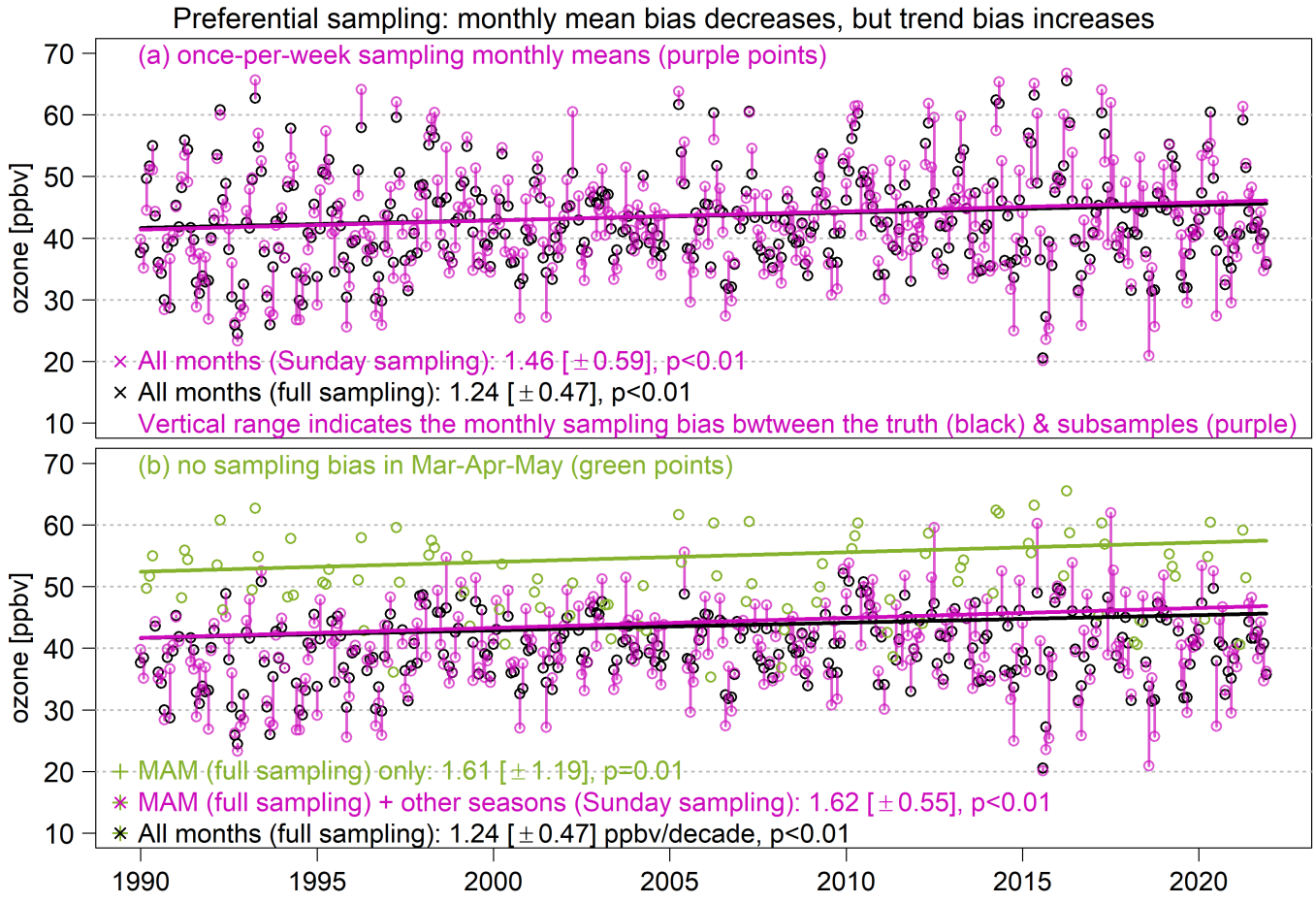

Figure S-12: Same as Figure S11, but replacing Friday with Sunday.

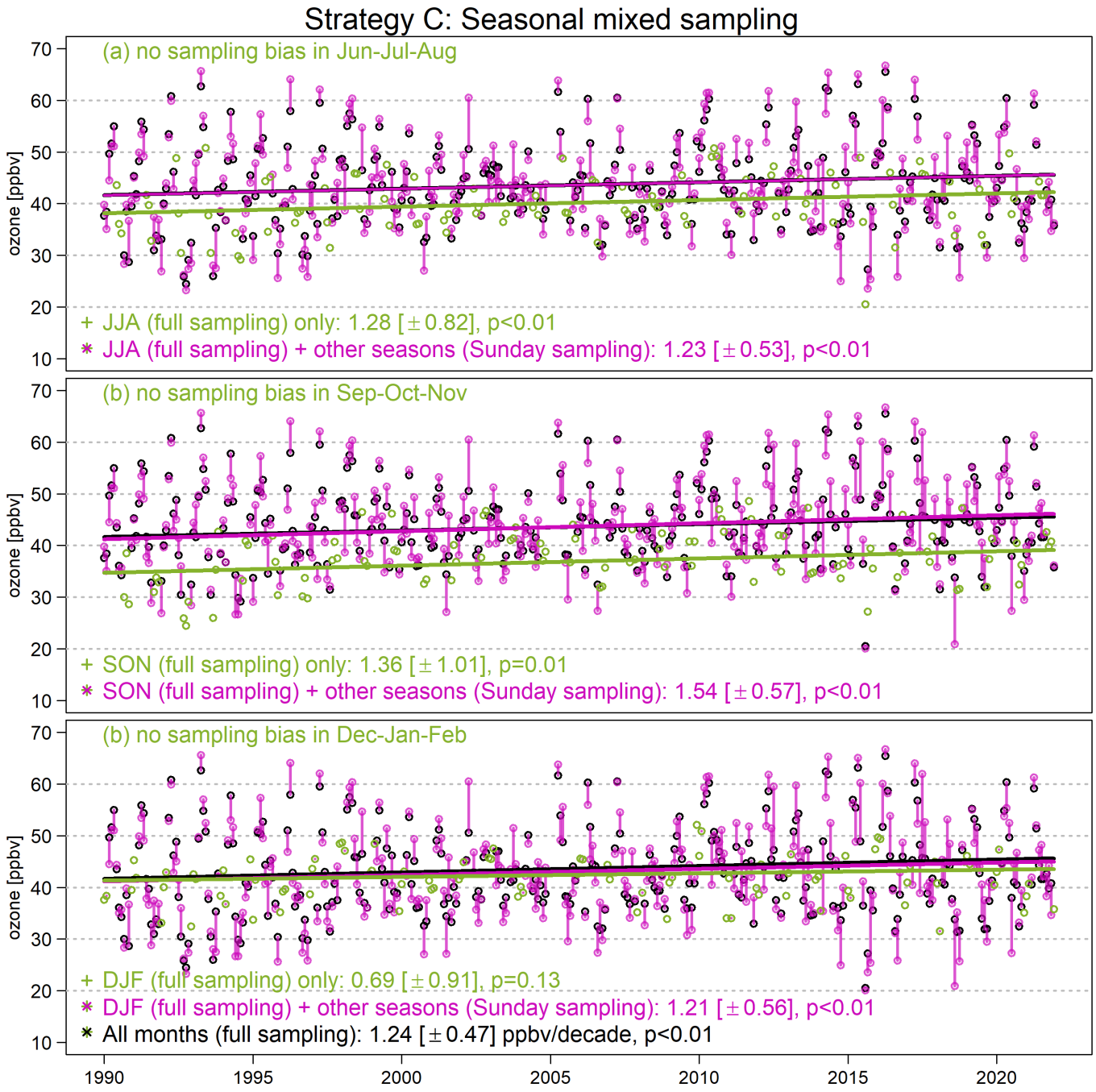

Figure S-13: Same as Figure S12, but replacing MAM with other seasons.

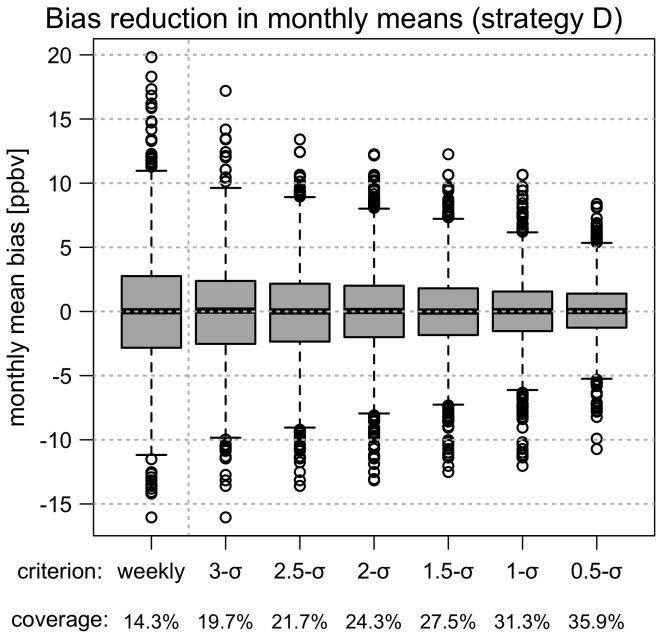

Figure S-14: Monthly mean bias (in units of ppbv) for Strategy D: Result is based on at most 3 samples per week scenario and different tolerance ranges (MLO nighttime ozone, 1990-2021).

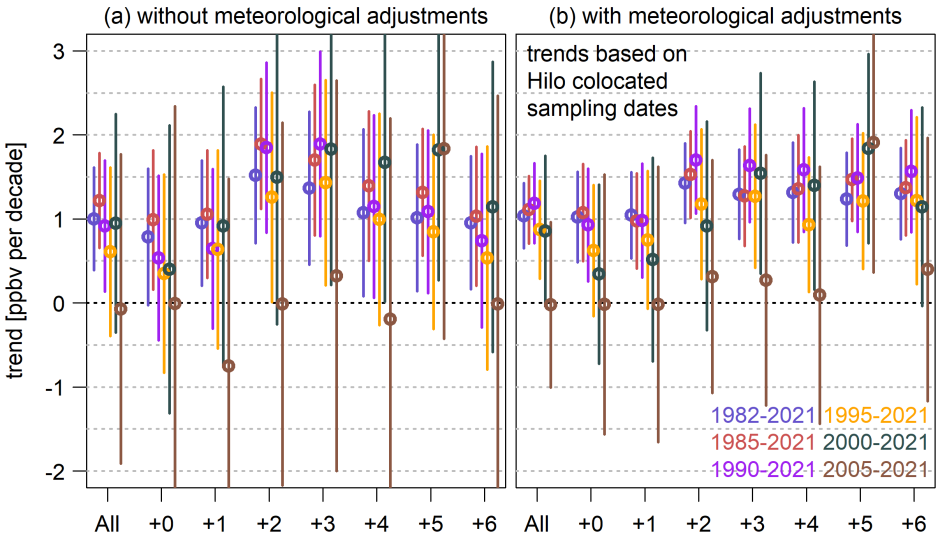

Figure S-15: MLO ozone trends based on Hilo ozonesonde sampling dates (labeled as +0), where +1 indicates the trends based on data taken from one day after Hilo ozonesonde sampling dates, and so on.

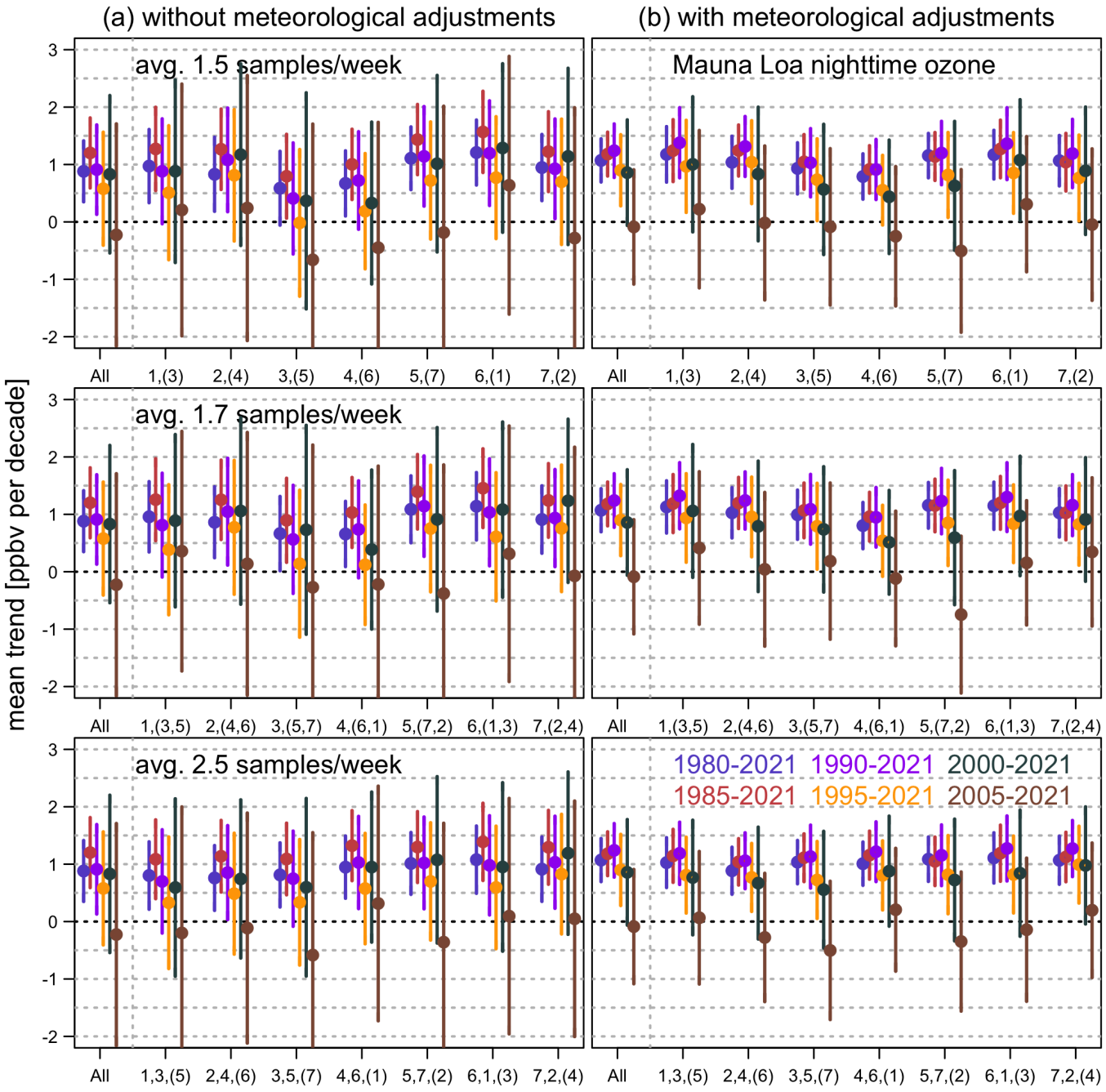

Figure S-16: Same as Figure 10, but based on the 1(+1):2σ, 1(+2):2σ and 2(+1):2σ schemes.